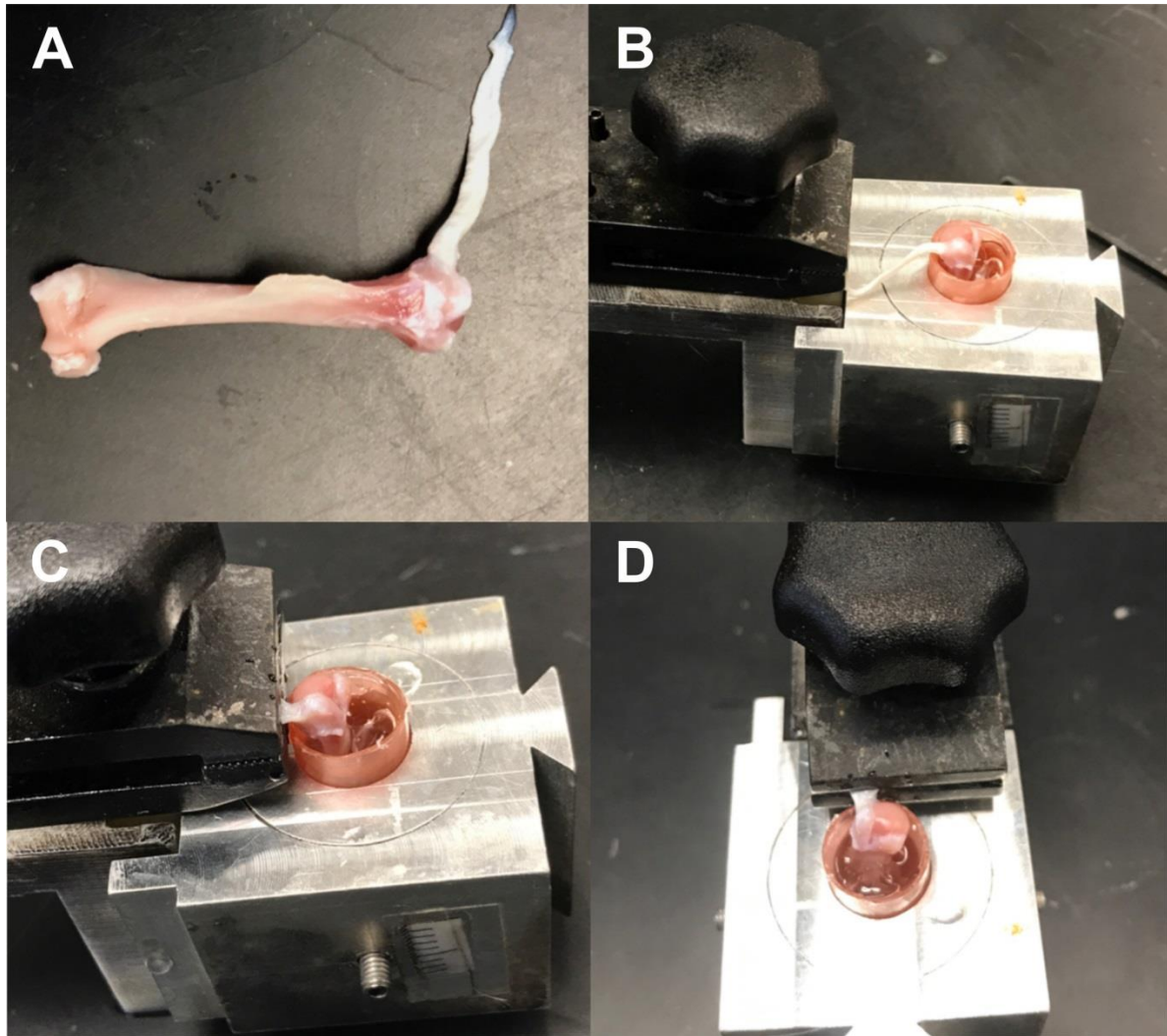
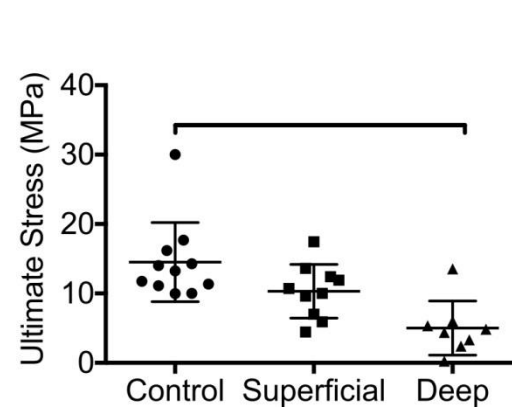
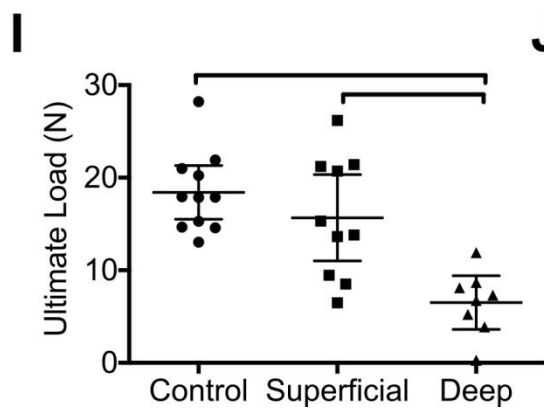
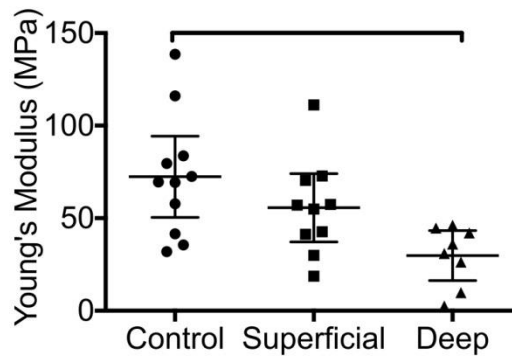
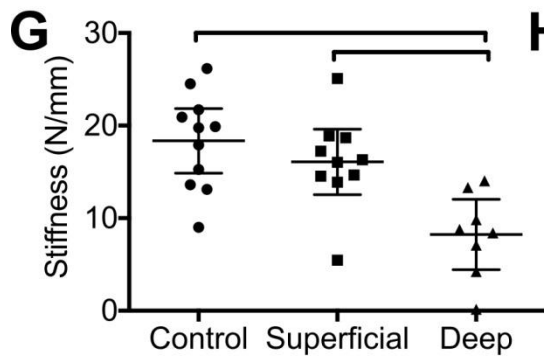
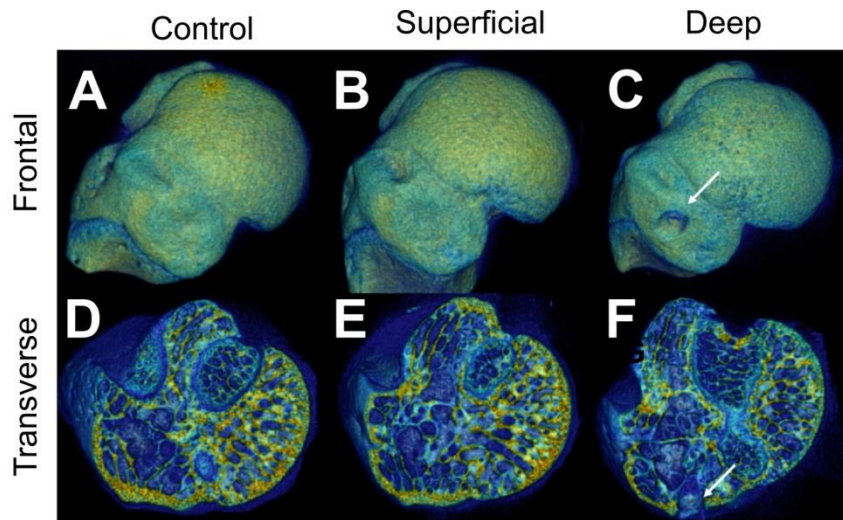


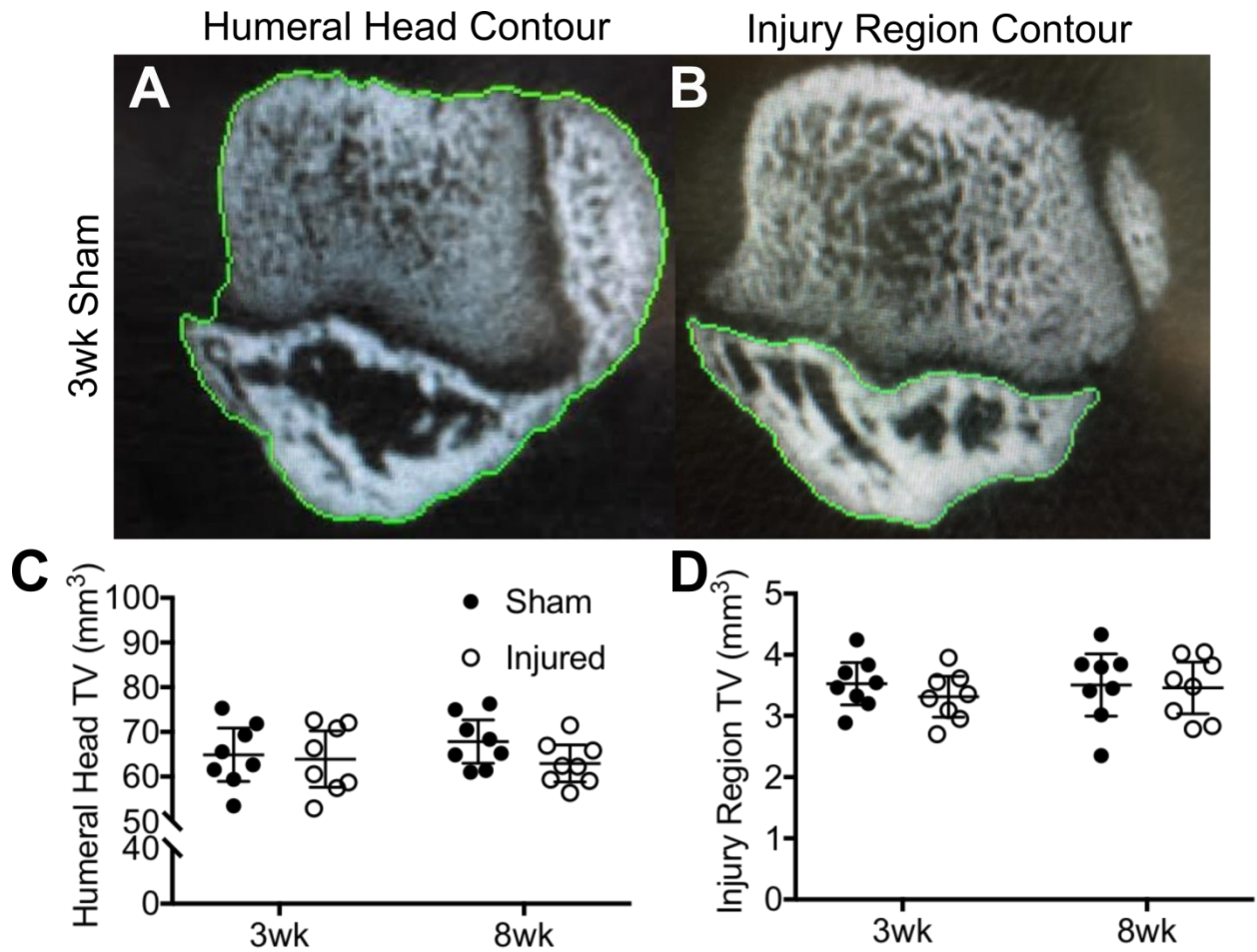
**Supplemental Figure 1. Injury model.** 1cm skin incision was made craniolaterally to the shoulder joint (A), along with a 0.5cm incision through the deltoid (B) to visualize the IS attachment to the humeral head (C) and implementation of the injury at the center of the IS attachment via a 0.3mm punch biopsy (D).



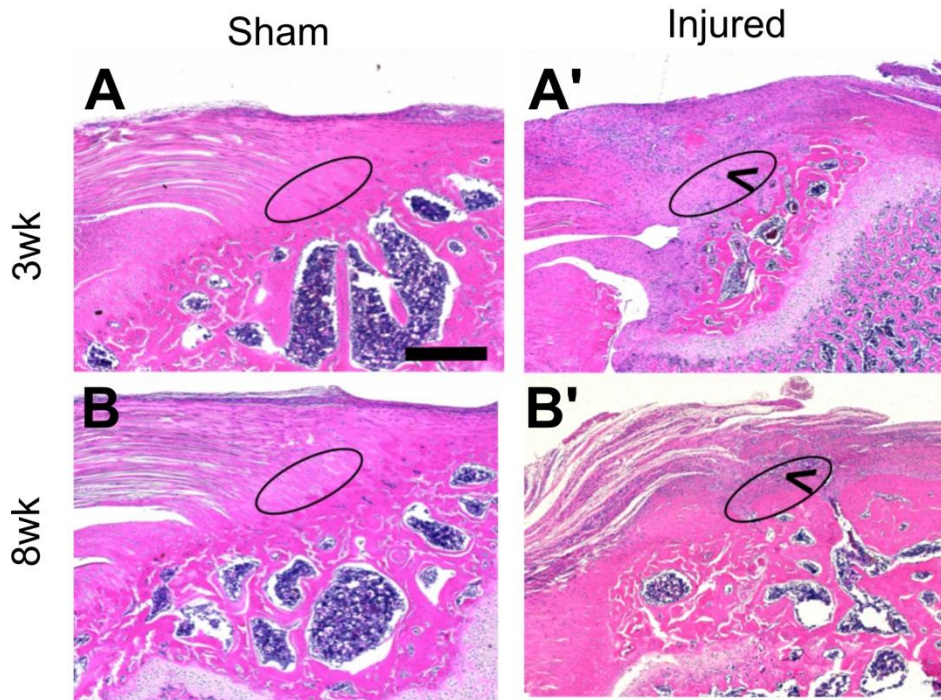
**Supplemental Figure 2.** (A-D) Mechanical testing setup for ex vivo validation of the injury. (A) Dissected humeri with intact IS tendons were stored in PBS-wrapped gauze for no more than 48hrs prior to testing. (B) The humeri were potted in polymethylmethacrylate in 2ml microfuge tubes and secured in a custom-built fixture. (C) Thin-film grips were used to grip the IS tendon near the insertion and (D) allowed for self-alignment of the thin-film grips for uniaxial loading.



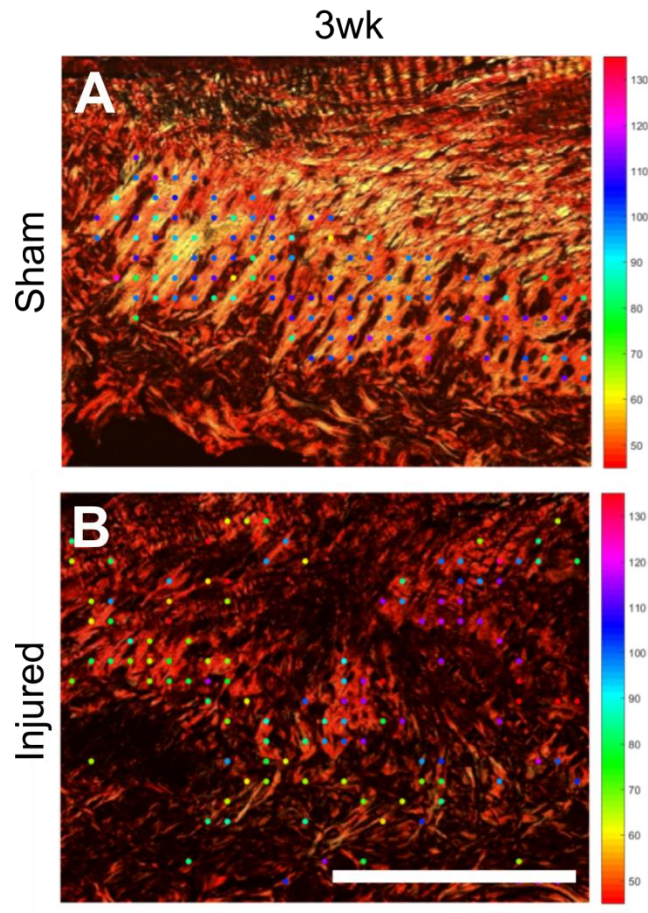
**Supplemental Figure 3. *Ex vivo* validation of rotator cuff injuries using microCT and biomechanics:** (A-F) MicroCT reconstructions of control, superficial injury and deep injury forearms. (A-C) Frontal plane views of microCT reconstructions showing the IS ridge of the humeral head for (A) Control, (B) Superficial injury, and (C) Deep injury attachments. (D-F) Transverse cut-plane (D) Control, (E) Superficial Injury, and (F) Deep injury. White arrowheads: Cortical bone injury in the injury region. (G) Stiffness, (H) Young's modulus, (I) ultimate load, and (J) ultimate stress of the IS attachment for Control, Superficial injuries, and Deep injuries at time zero. Bars indicate significant differences between groups. Ultimate load and stiffness were significantly reduced for the IS attachments with Deep injuries compared to Superficial injuries or controls. Young's modulus and ultimate stress were significantly reduced for Deep injuries compared to control group. No significant differences were observed between groups for ultimate strain and toughness; p-value < 0.001, ANOVA.



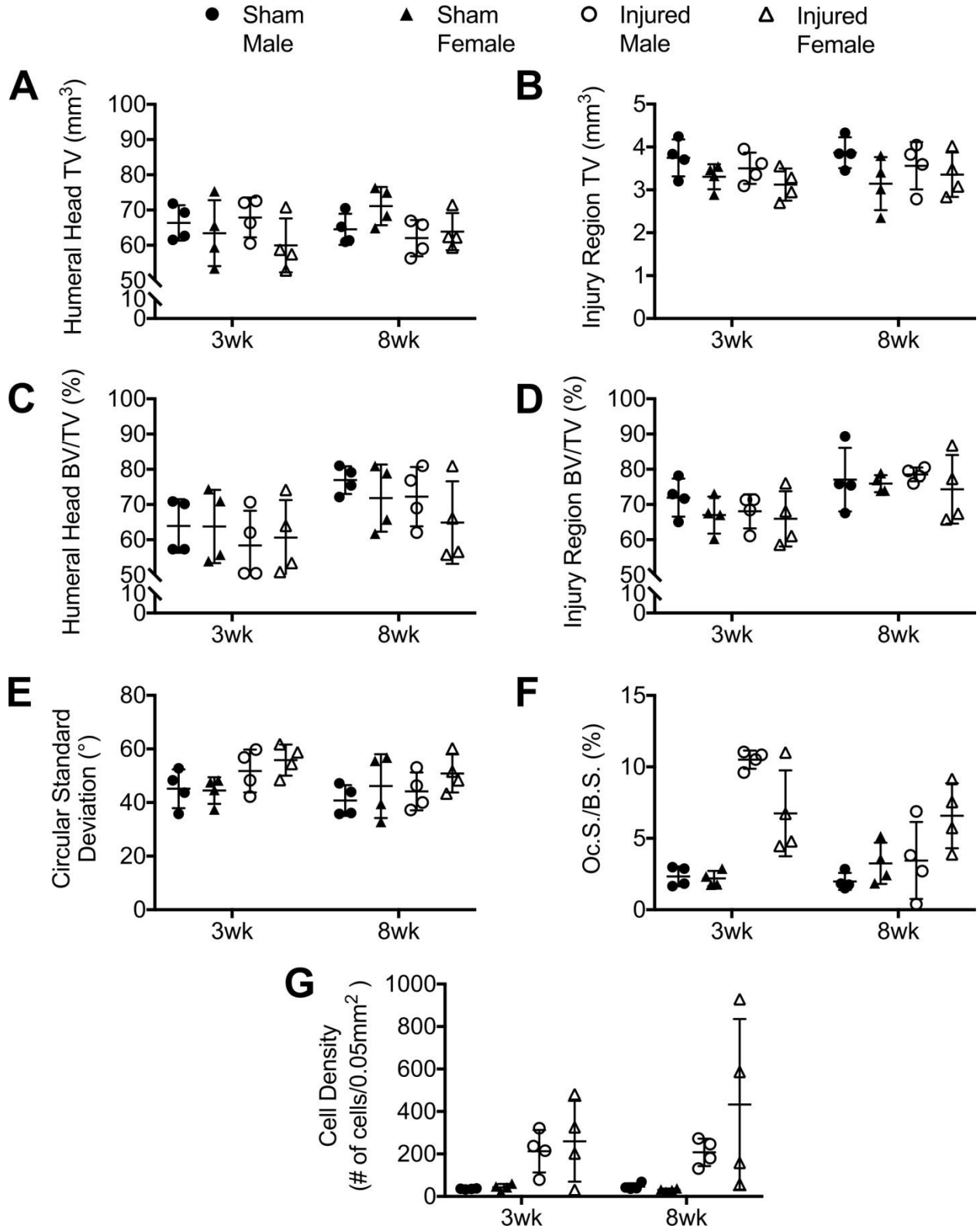
**Supplemental Figure 4. MicroCT contouring for humeral head and injury regions with no significant differences in humeral head or injury region total volume.** (A-B) Representative contours for (A) humeral head and (B) injury region total volume and bone volume analyses. (C) Humeral head TV and (D) Injury Region TV for 3wk control, 3wk injured, 8wk control, and 8wk injured attachments. Bars indicate significant differences between groups ( $p < 0.05$ , mean  $\pm$  95% CI).



**Supplemental Figure 5. (A-B') H&E 5x-magnification transverse histological images of (A) 3wk sham, (A') 3wk injured, (B) 8wk sham, and (B') 8wk injured. Black arrowheads point to cell infiltration of injury at 3wks and 8wks. Scale bar: 200 $\mu$ m. The ellipse represents the area of the attachment evaluated for cellularity across all attachments using a custom MATLAB script.**



**Supplemental Figure 6. (A-B)** Picrosirius Red 10x-magnification MATLAB code representative bundle locations of (A) 3wk sham and (B) 3wk injured attachments.



**Supplemental Figure 7. Three-way ANOVA graphical representations to identify sex differences, with no significant differences seen.** (A) Humeral head TV, (B) Injury Region TV, (C) Humeral Head BV/TV, (D) Injury Region BV/TV, (E) Collagen Alignment, (F) Oc.S./B.S., and (G) Cell Density for 3wk male sham, 3wk female sham, 8wk male sham, 8wk female sham, 3wk female injured, 3wk male injured, 8wk female injured, and 8wk male injured attachments.